IVO PASEKA

Institute of Inorganic Chemistry, Academy of Sciences of the Czech Republic, Rež, Czech Republic

SCIENTIFIC PAPER

541.135.5+546.96+
+54-31:546.11:541.183

CHARACTERIZATION OF RuO_2, Ru AND $Ru_{0.3}Ti_{0.7}O_2$ MATERIALS AND THEIR BEHAVIOUR IN HYDROGEN EVOLUTION REACTION

Polarization characteristics of the hydrogen evolution reaction were studied at RuO_2, $Ru_{0.3}Ti_{0.7}O_2$ and Ru electrodes prepared by various methods. The initial activity of all oxide electrodes, related to the real surface area, was comparable. After a long–term cathodic loading of electrodes the change of physical–chemical properties occurred. Voltammetric curves of electrodes showed that ad– and absorption of hydrogen occurred after a long–term cathodic loading. Absorbed hydrogen caused changes of RuO_2 lattice parameters and even changes of lattice parameters of the Ti support on which the RuO_2 layer was deposited. Arisen stresses in the Ru – oxides layers caused the destruction of the electrode layer and limited life–time of these electrodes.

Key words: Ruthenium oxides, electrodes, hydrogen evolution, hydrogen absorption, hydrogen adsorption.

Ceramic oxides have been employed in electrochemistry as an outstanding electrode material for a long time. They serve as anodes in chlorine production [1,2] or in other chemical applications where oxygen is evolved. A great interest has also been devoted to the ceramic electrodes as cathodes in hydrogen evolution reaction (HER) [3,4]. A recently increased number of reports on electrocatalytic and physical–chemical characteristics have demonstrated this renewed interest. Especially RuO_2 belongs to these oxide materials. Its characteristics were studied both in acid [5–9] and alkaline environment [10–14]. These materials were also used as cathodes in standard chlorate electrolyte [10,11] in aim to successfully replace commonly used steel cathodes.

Various electrochemical techniques were employed for the complete RuO_2 characterization, i.e. voltammetry, chronoamperometry, measurement of pseudo–stationary current – potential curves, and A.C. impedance spectroscopy [15–18]. Electrochemical methods were mostly complemented with various physical methods, e.g. SEM microscopy, XPS spectroscopy, X–ray diffractometry, Auger spectroscopy, and AFM [5–14, 19–21]. It has been concluded that there is a possibility to prepare RuO_2 electrode with a developed surface, where hydrogen is evolved with a particularly low overpotential. Furthermore, in contrast to the other active electrodes, e.g. the electrodes based on Ni, the Ru–based electrodes are resistant to the known electrode poisons like copper, iron, and mercury. This feature was explained on the assumption that RuO_2 is not reduced into metallic ruthenium during the HER. This explanation was also supported by XPS analyses [5,8]. Nevertheless, the fact that the HER proceeds on the oxide material, thermodynamically unstable in the potential interval studied, is rather unexpected. The observation that the activity of RuO_2 electrodes increases with prolonging time of the HER [7,8] indicates some surface changes of RuO_2 electrodes. Takasu and Murakami [21] and later Blouin and Guay [8,20] described a charge increase during voltammetry and showed that this increase was induced by a long–term cathodic polarization of thermally prepared RuO_2 electrodes. The phenomenon was explained by increased wet ability of hydrophobic surface sites on the oxide caused by its surface hydroxylation. Blouin et al. [8] presumed that the hydroxylation is accompanied by the hydrogen chemisorption into the structure of a host material and by an increased number of active centres, which are responsible for the hydrogen generation. Already Trasatti [9] supposed that atomic hydrogen could penetrate to some extent in the structure of the RuO_2 oxide material. The direct evidence of incorporation hydrogen in the RuO_2 structure was done in papers [22,23]. Y. Mo et al. [22] showed by *in situ* Ru K–edge X ray absorption fine structure (XAFS) measurement that during the hydrogen evolution reaction an increase of Ru–O bond length occurred. Chabanier et al. [23] studied the changes of RuO_2 structure during the hydrogen evolution by electrochemical *in situ* X–ray diffraction measurements. It followed from the paper that an increase of the lattice constant of the tetragonal structure of RuO_2 occurred during the hydrogen evolution. This change in the lattice parameter was explained as a result of the hydrogen absorption in the oxide layer. It also followed from the paper that these structure changes were not totally reversible. Hydrogen ingress in the layer caused the poor mechanical stability of RuO_2 electrodes. Also Chen et al. [20] by AFM measurements proved a deformation of RuO_2 layer during the hydrogen evolution as a result of hydrogen penetration in the oxide layer. This deformation resulted in an increase of the effective surface are of the RuO_2 electrodes by about 20 to 30%.

Author address: Institute of Inorganic Chemistry, Academy of Sciences of the Czech Republic, 250 68 Rež, Czech Republic
Paper received and accepted: May 3, 2005

EXPERIMENTAL PART

Electrode preparation

A commercial titanium (99.5%) wire (diameter 0.9 mm) was used as a support for the ruthenium layers. Before the layer deposition, the wire was first degreased with acetone and ethanol and then etched in boiling 23% HCl for 30 min. In some cases a gold wire (diameter 1.0 mm) instead of titanium was used as a support for RuO_2 layers. The electrode layer was prepared by dipping the preconditioned wire into the dipping solution.

RuO_2 electrodes were prepared by dipping of a wire into a 0.2 M $RuCl_3$ solution acidified with few drops of HCl. An adhered solution was dried at 100°C for 5 min and then calcined 10 min at 350°C or 430°C. The electrodes were finally annealed at 350°C or 430°C for 1h in air or in oxygen atmosphere.

The $Ru_{0.3}Ti_{0.7}O_2$ electrodes were prepared by a method described by Forti et al. [24], where the precursor polymer solution was prepared by mixing citric acid (CA) in ethylene glycol (EG) at 65°C. After the complete dissolution of CA, the temperature was increased to 90°C and titanium isopropoxide (TI, Aldrich) was added in a molar ratio CA : EG : TI = 4 : 16 : 1. The preparation was finished by adding of 0.2 M solution of $RuCl_3 \cdot nH_2O$ in HCl (1:1). The electrode layer was prepared again by dipping of a titanium wire in the solution. After each dipping step, the adhered layer was dried at 100°C and calcined at 400°C for 15 min. After the application of all required layers, the electrode was finally annealed at 400°C in air or in the oxygen flow for 1 hour.

RuO_2 electrodes (B – type) were deposited also on the TiO_2 porous substrate. This porous layer was prepared from precursor polymeric solution, prepared by a method analogous to previous, but using a solution without $RuCl_3$. After each dipping step, a layer was dried at 100°C for 10 min and then calcined at 400°C for 15 min. This procedure was repeated ten times. For the final calcination, the electrode was heated at 400°C in an oxygen flow for 1 hour. For preparing the RuO_2 layers, the prepared support was immersed into a solution of 0.2 M $RuCl_3$ acidified with HCl. An adhered solution was dried at 100°C for 10 min and then calcined at 400°C in air for 15 min. The procedure was repeated according to the number of layers required. The final calcination was carried out at 400°C in air or oxygen flow for 1 hour.

Ru electrodes were prepared as RuO_2 ones but thermal processing was carried out in the hydrogen flow at 200°C or 400°C.

Diffraction patterns were collected with diffractometer PANalytical X'Pert PRO equipped with conventional X–ray tube (Co Kα radiation, 40 kV, 30 mA, point focus), X–ray monocapillary with diameter of 0.1 mm, and multichannel detector X'Celerator with an anti–scatter shield. A sample holder for single crystal XRD measurement was adopted by adding z–(vertical) axis adjustment. To align a sample for in–plain diffraction and for choosing measurement points the detector is replaced with a light. The XRD patterns were taken between 25 and 100° 2Θ with 0.0167° step and 2300 s counting time per step.

Electrochemical measurements

Polarization and voltammetric curves were measured in a common three–electrode cell. Pseudo–stationary polarization curves were obtained by the galvanostatic method. All potential values were corrected by subtracting the ohmic *iR*–drop between reference and working electrodes. Electrode potentials were determined against reference hydrogen electrode (*rhe*) in the same solution and they are also given against *rhe*. The ohmic *iR*–drop between reference and working electrodes was measured by the interruption technique and its values were registered with a digital oscilloscope Tektronix TDS 210. Voltammetric curves were obtained by potentiostat Wenking ST 72 linked with a generator of triangular voltage and a PC.

All measurements were carried out in 1M H_2SO_4 solution. The solution was deoxygenated before experiments by bubbling with purified nitrogen.

RESULTS

Polarization curves

The example of polarization curves of the RuO_2 electrode (calcination temperature 430°C, 18 layers) is given in Fig. 1. Curve 1 represents the electrode after the preparation. Curve 2 shows the polarization curve after the activation by cathodic current density (related to the geometric surface area) $I = 0.25$ A cm^{-2} for 17h. In accordance with results presented in previous papers a significant increase in the activity is apparent after this activation. Even more considerable increase in the activity occurred after the oxidation at the potential around $E \approx 1.0$ V. Curve 3 represents the polarization curve measured after this anodic activation. The increased activity caused by the anodic activation is not permanent, however. A gradual increase in the potential occurred during continuing hydrogen evolution reaction at the current density $I = 0.25$ A cm^{-2}. Curve 4 represents the electrode behaviour after the anodic activation which was followed by 20h hydrogen evolution at named current density. Further slow decrease in the activity was apparent during continuing hydrogen evolution. This is shown by Curve 5 in Fig. 1.

Polarisation curves of RuO_2 electrodes deposited on Au wire (the preparation technique was identical with RuO_2/Ti preparation) are depicted in Fig. 2. On the contrary to the RuO_2 electrodes deposited on the Ti wire, no marked decrease was observed in the electrode activity of long–term loaded electrodes, however. The

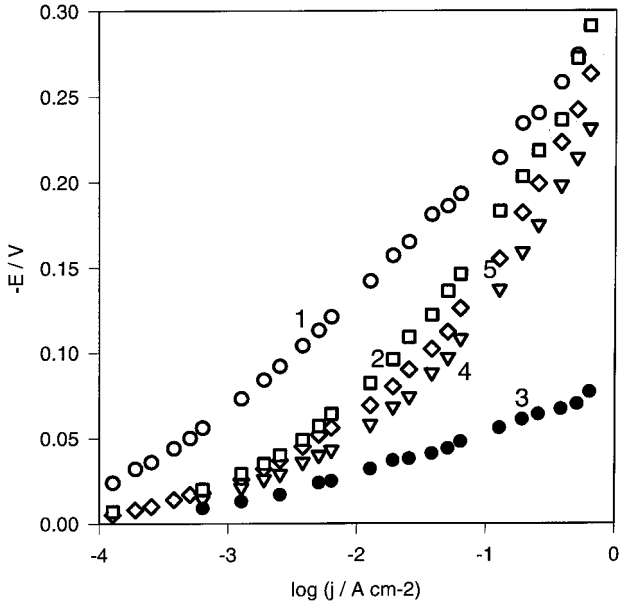

Figure 1. Polarization curves for the HER on RuO_2 electrode deposited on Ti wire (18 layers). Curve 1 – after the electrode preparation, 2 – after cathodic loading by I = 0.25 A cm^{-2} for 17.5 hours, 3 – after 2 and anodic oxidation at E = 1.035 V, 4 – after 3 and additional cathodic loading by I = 0.25 A cm^{-2} for 20 h (together 37.5 h), 5 – after 4 and additional cathodic loading for 18.5 h (together 56 h).

activity for the HER increased continuously even after 157 h of cathodic loading. The polarisation curve of this

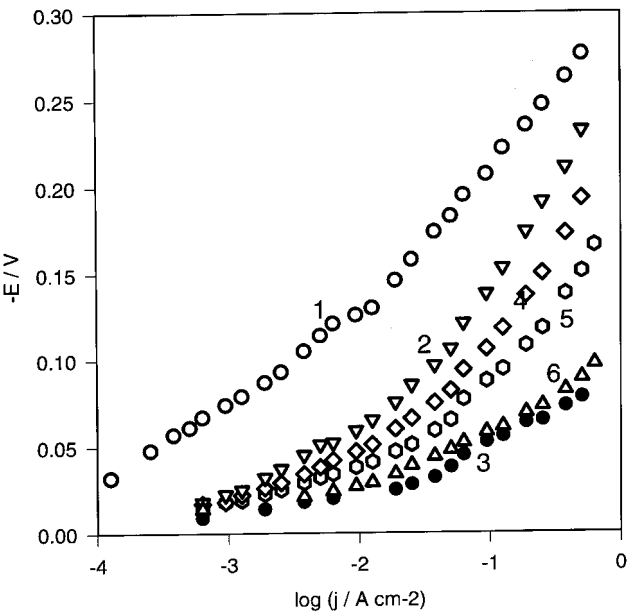

Figure 2. Polarization curves for the HER on RuO_2 electrode deposited on Au wire (18 layers). Curve 1 – after the electrode preparation, 2 – after cathodic loading by I = 0.25 A cm^{-2} for 18 hours, 3 – after 2 and anodic oxidation at E = 1.035 V, 4 – after 3 and additional cathodic loading by I = 0.25 A cm^{-2} for 22 h (together 40 h), 5 – after 112 h of cathodic loading, 6 – after 153 h of cathodic loading.

long-term loading electrode approaches to that registered after anodic activation.

Polarization curves of the HER on the RuO_2 electrodes calcined at 350°C are similar as those calcined at 430°C. Their activity also depends on the time of cathodic loading and it considerably increased after the anodic oxidation. Polarization curves of the HER on $Ru_{0.3}T_{0.7}O_2$ and RuO_2 electrodes deposited on the porous TiO_2 substrate are similar to those shown in Fig. 1. Only the activation and also the deactivation during the cathodic loading proceeded more quickly.

The overview of the polarization features of electrodes prepared by all methods with corresponding number of deposited layers is given in Table 1.

Ru electrodes behave quite differently. The polarization curve of the electrode measured after the preparation is displayed in Figure 3, Curve 1. The electrode is extraordinarily active, as indicated by the value $I_{-0.2V}$ exceeding 1 A cm^{-2}. The polarization curve is characterized by a low slope b ≈ 0.025 V. When the electrode has been loaded for some time by cathodic current density of I = 0.25 A cm^{-2}, its activity moderately decreases, which is mainly obvious on the polarisation curve at high current density I ≥ 0.2 A cm^{-2}. However, the value of $I_{-0.2V}$ remains still very high ($I_{-0.2V}$ > 1 A cm^{-2}). The considerable decrease in the activity of the HER occurred after several-hour loading by cathodic current density of 0.25 A cm^{-2}. The polarization curve of the electrode after 17 hours loading shows Curve 3. In the region of low current density (I < 0.01 A cm^{-2}), the current density of deactivated electrode is by an order of magnitude lower at a corresponding potentials than on a

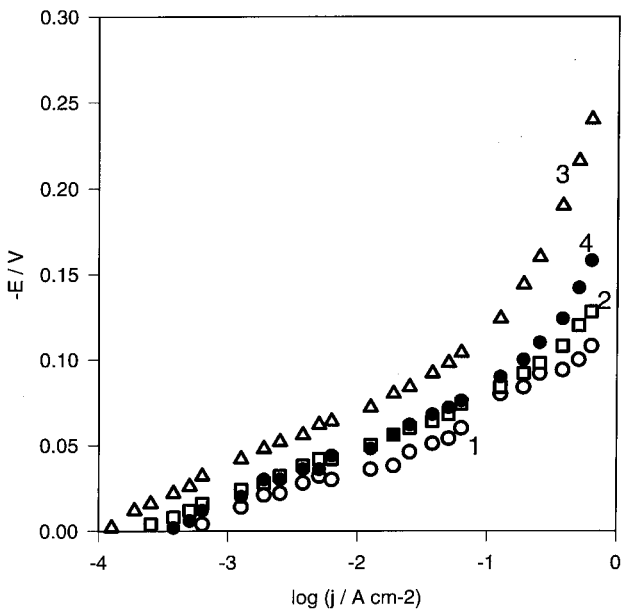

Figure 3. Polarization curves for the HER on Ru electrode. Curve 1 – after the electrode preparation, 2 – after cathodic loading by I = 0.25 A cm^{-2} for 1 h, 3 – after 19 h of cathodic loading, 4 – after 3 and anodic oxidation at E = 0.70 V.

Table 1. Summary of the ruthenium electrode properties

Electrode	RuO_2 I	RuO_2 II/Au	$Ru_{0.3}Ti_{0.7}O_2$	RuO_2/TiO_2	Ru/TiO_2	Ru/TiO_2
n	8	18	10	10	4	4
$t_{cal.}$/°C	350	450	400	400	200	400
I	1200	92	307	55.3	>1000	>1000
f	1363	23	240	65		
j	0.9	4.0	1.5	0.85	>12*	>14*
I_{1h}	1790	165	1544	171	>1000	355
f_{1h}	2004	39	280	128		
j_{1h}	0.9	4.2	5.5	1.35	>12*	5*
$I_{(xh)}$	>>1000(22)	171(17)	386(20)	43(23)	164(17)	81(20)
$f_{(xh)}$	2580(22)	76(17)	260(20)	153(23)	84(17)	71(20)
$j_{(xh)}$		3.8(17)	1.4(20)	0.27(23)	1.9(17)	1.2(20)
$I_{(xh)}$	2500(137)	31330(153)				
$f_{(xh)}$	3400(137)	142(153)				
$j_{(xh)}$	0.73(137)	219(153)				
remark		layer deposited on Au			*f measured after 17h	*f measured after 20h

List of symbols and abbreviation: n – number of layers, I – current density of the HER at E = –0.20 V related to the geometrical surface area, f – roughness factor evaluated from the VCs, j = I/f, I_{1h} – c.d. of the HER after 1h loading of the electrode by I = 0.25 A cm^{-2}, f_{1h} – f after 1h loading by the named c.d., $j_{1h} = I_{1h}/f_{1h}$, $I_{(xh)}$, $f_{(xh)}$, $j_{(xh)}$ - quantities defined above, measured after x hours of cathodic loading (they are quoted in parentheses).

new electrode. At higher current densities, the decrease in the current density at corresponding potentials is even much higher. It is the result of the fact that the slope of the polarization curve at those higher current densities is higher (b ≈ 0.156) than at the low densities (b ≈ 0.032). It is noteworthy that polarization behaviour of the deactivated electrodes depends significantly on the electrochemical pre–treatment of the electrode surface. The deactivated electrode can be partly activated by a short–term – only several minute anodic polarization at around E ≈ 1.0 V. The polarization curve of such activated electrodes is represented by Curve 4.

The overview of the polarization features of the electrode is also given in Table 1.

Voltammetry in the potential region 1.04 to 0.45 V

The voltammetric curves (VCs) of RuO_2 electrodes (430°C, 18 layers) before cathodic loading (Fig. 4) are similar with VCs shown in the papers mentioned in Introduction e.g. [8,9,15,21]. The charges of anodic Q_o and cathodic Q_R branches of VCs measured with low sweep rate (ν < 0.4 mV s^{-1}) are almost identical, but at higher ν their values depend on the sweep rate. The value of $(Q_A + Q_R)/2$ decreased with increasing of the sweep rate. Also the ratio Q_A/Q_R changed with various sweep rate. We measured Q_A and Q_R at three various sweep rates (ν = 4.34, 1.76 and 0.43 mV·s^{-1}). The measured $(Q_A+Q_R)/2$ values were extrapolated to ν = 0 and by this way the extrapolated Q_{ex} was found. This quantity was then used for the evaluation of the roughness factor of the individual electrodes. The specific charge value Q = 0.86 C·m^{-2} (ΔE = 0.604 V) was used as a reference charge in agreement with the value published previously [15].

The roughness factor of Ru electrodes was also evaluated from voltammetric curves. The Q_{ex} values obtained by this way were divided by factor 3.5 as we found [25] that $(Q_A+Q_R)/2$ values for Ru blacks are about 3.5 times greater than for RuO_2 blacks.

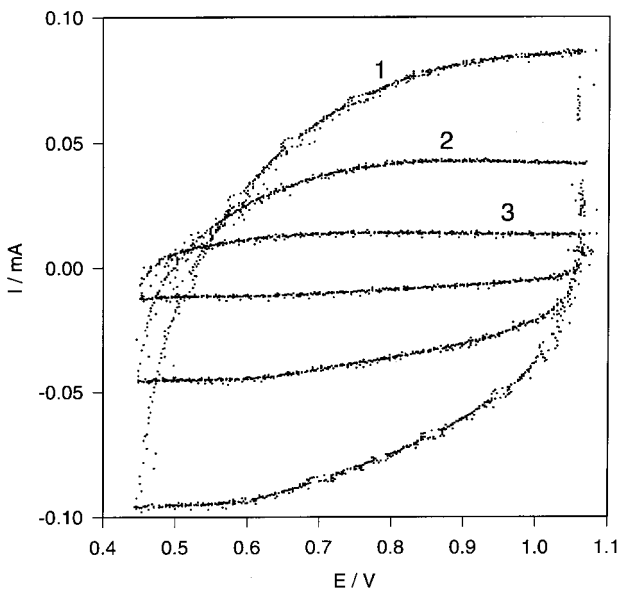

Figure 4. Voltammetric curves of RuO_2 electrode (8 layers). Influence of the sweep rate. Curve 1 – ν = 4.34 mV s^{-1}, 2 – ν = 1.76 mV s^{-1}, 3 – ν = 0.43 mV s^{-1}.

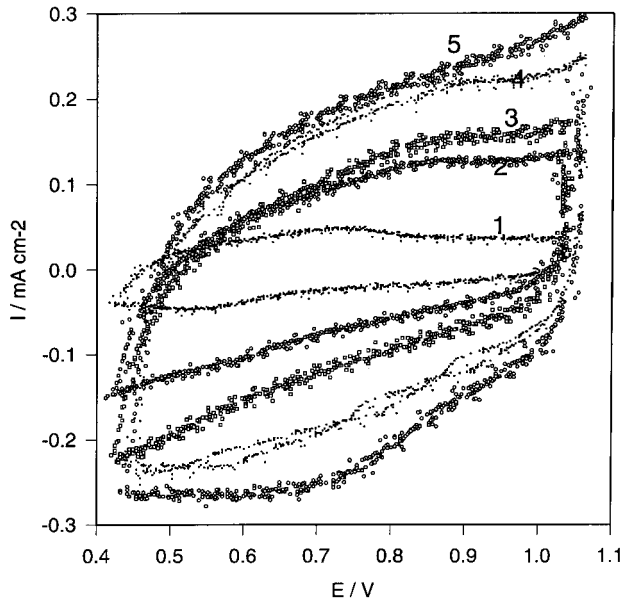

Figure 5. Influence of cathodic loading time on VCs. RuO_2 electrode deposited on Au wire (18 layers), ν = 4.34 mV s^{-1}. Curve 1 – after the electrode preparation, 2 – after cathodic loading by I = 0.25 A cm^{-2} for 18 h, 3 – after 40 h of cathodic loading, 4 – after 118 h of cathodic loading, 5 – after 153 h of cathodic loading.

The influence of electrode polarisation by cathodic current density I= 0.25 A·cm^{-2} for various time on voltammetric curves is shown in Figs. 5 and 6. Fig. 5 shows that the currents in both branches of voltammetric curves gradually increase with increasing time of cathodic polarisation. If the increase in voltammetric current after 153 hours polarisation by cathodic current is caused by a surface area enlargement only, then the electrode surface area increased by a factor about 6.5.

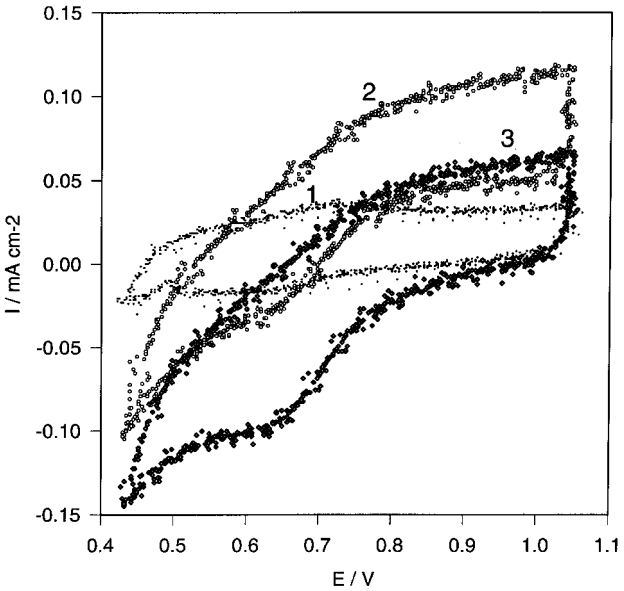

Figure 6. Voltammetric curves of RuO_2 electrode deposited on Ti wire (18 layers). Influence of cathodic loading time. Curve 1 – after the electrode preparation, 2 – after 20 h of cathodic loading by I = 0.25 A cm^{-2} and anodic oxidation at E = 1.035 V for 30 min., 3 – after 2 and additional oxidation at E = 1.035 V for 90 min.

A different shape of VCs was observed on RuO_2 electrode deposited on Ti wire (Fig. 6). While VC of the electrode measured after the preparation is identical with that depicted in Fig. 5 Curve 1, VC of electrode which was cathodic loaded for 17.5 h with I = 0.25 A cm^{-2} was quite different than corresponding one shown in Fig. 5 Curve 2. The shape of the Curve 2 in Fig. 6 is appreciably influenced by faradaic anodic current. This current shifted voltammetric curve in the direction of anodic current. After prolonged pre-polarisation of the electrode at E = 1.04 V for 90 min. before the voltammetric measurement the currents in the anodic branch of VC appreciably decreased. Nevertheless the shape of VC is still different from corresponding curve in Fig. 5.

Voltammetry in the potential interval from 0.005 to 0.70 V

Voltammetric curves of RuO_2 electrode deposited on Au wire and measured after various time of cathodic polarization are shown in Figs. 7. In Fig. 8 there are shown VC curves of electrodes which were also cathodic loaded, but in addition, before VC measurement they were anodic activated at E = 1.04 V.

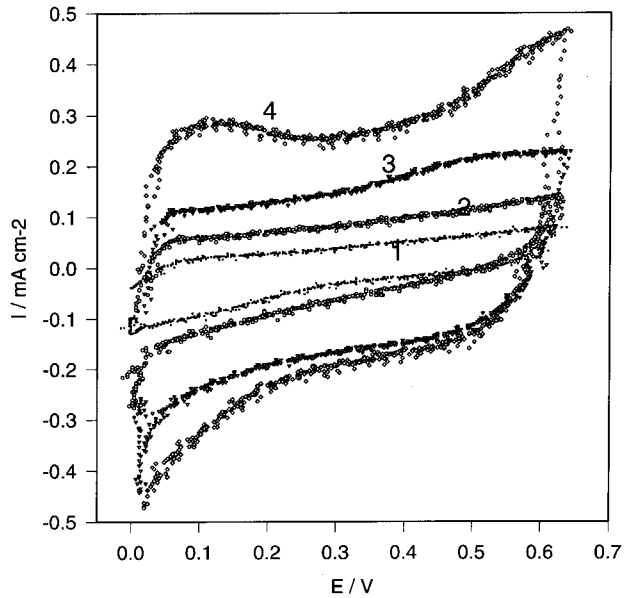

Figure 7. Voltammetric curves of RuO_2 electrode deposited on Au wire (18 layers). Potential range 0.005–0.65 V. Influence of cathodic loading time. Curves were recorded after indicated loading time LT in hours. Number in parenthesis (E0.25) represents the electrode potential at the cathodic current density I = 0.25 A cm^{-2}. ν = 4.34 mV s^{-1}. Curve 1 – LT = 0 (E0.25 = –0.308 V), 2 – LT = 1.6 ($E_{0.25}$ = –0.225 V), 3 – LT = 18 ($E_{0.25}$ = –0.227), 4 – LT = 40 ($E_{0.25}$ = –0.186), 5 – LT – 153 ($E_{0.25}$ = –0.113).

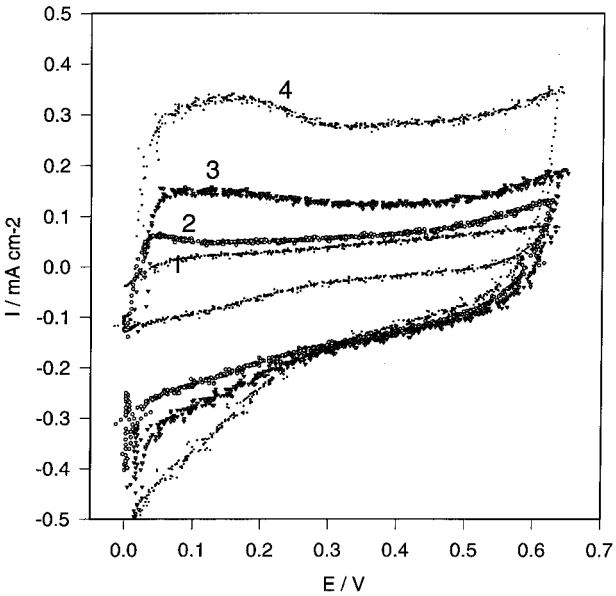

Figure 8. Voltammetric curves of RuO_2 electrode deposited on Au wire (18 layers). Potential range 0.005–0.65 V. Influence of cathodic loading time. Curves were recorded after indicated loading time LT in hours and anodic oxidation at E = 1.035 V. Number in parenthesis ($E_{0.25}$) represents the electrode potential at the cathodic current density I = 0.25 A cm^{-2}. ν = 4.34 mV s^{-1}. Curve 1 – LT = 0 ($E_{0.25}$ = –0.308 V), 2 – LT = 18 ($E_{0.25}$ = –0.150), 3 – LT = 40 ($E_{0.25}$ = –0.100 V), 4 – LT = 153 ($E_{0.25}$ = –0.100 V).

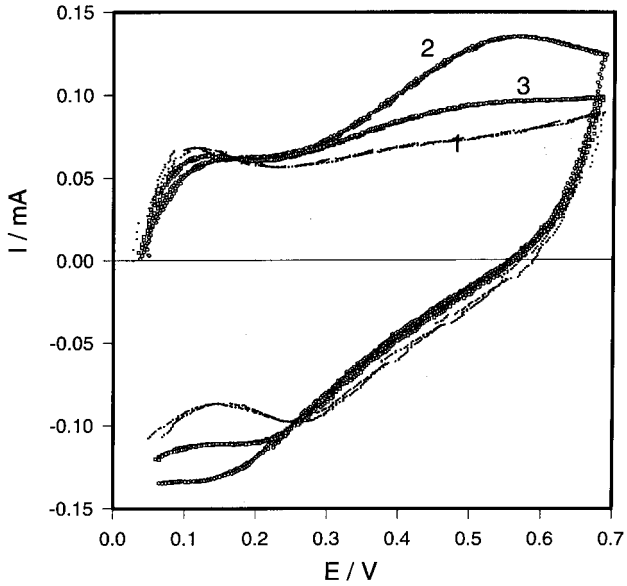

Figure 9. Voltammetric curves of Ru electrode deposited on Ti wire (6 layers). Curve 1 – after the electrode preparation, 2 – after cathodic activation by I = 0.25 A·cm^{-2} for 1 h, 3 – measured immediately after curve 2.

In the legend for illustrations of both figures there are given the current density values of the HER measured at E = –0.10 V shortly before VC measurements. In both cases, before each VC measurement, the RuO_2 electrodes were pre–polarized at E = 0.002 V for about 15 min. and than about 5 min. at E = 0.05 V. Voltammetric curves show that the activation of RuO_2 electrodes by hydrogen evolution causes the increase in the currents both in anodic and cathodic branches of VCs. The increase in currents caused by cathodic polarisation measured at about 0.30 V is roughly the same as that registered on VCs measured in the potential region between 1.04 and 0.43 V. It means that the rise in voltammetric currents at this potential was caused by the increase in the surface area of the RuO_2 electrode. Comparing Figs. 7 and 8, mainly their anodic branches, shows that the courses of VCs measured immediately after cathodic loading with those measured after anodic polarization (at about 1.04 V) are little different. The characteristic feature of VCs after anodic activation is lowering of anodic current in the potential range between 0.4–0.65 V and *vice versa* increasing of anodic current in the range of less positive potentials E between 0.02–0.3 V. The difference is the more obvious the longer the RuO_2 electrode is cathodicaly polarized. The comparison between the increase in the surface area (after 153 h loading the increase about 6) and the activity for the HER (expressed as $I_{-0.1V}$, the corresponding increase by about two orders) has shown that the increase in the activity for the HER is caused not only by the surface enlargement.

Voltammetric curves of $Ru_{0.3}Ti_{0.7}O_2$ electrodes are similar to those of RuO_2. The influence of the HER on the course of VC was followed only for considerably shorter time (17 h) and the Figure is not shown here.

Voltammetric curves of Ru electrodes are shown on Fig. 9. On the freshly prepared electrode it is seen a broad oxidation peak in the range of potentials between 0.05–0.22 V. After the cathodic activation of the electrode (I = 0.25 A cm^{-2}) the mentioned oxidation peak lowers and a new appreciably greater peak appears in the potential range between about 0.35–0.7 V. In the next run which followed immediately after the 2nd run, this peak appreciably decreased. The course of VCs of Ru/TiO_2 electrodes can be explained on the assumption that during the long–term cathodic polarization the hydrogen absorption in metallic lattice occurred. This absorbed hydrogen is oxidized in the second oxidation peak together with the ruthenium oxidation. In the following sweep (Curve 3) at a short–term cathodic polarization hydrogen was not able to accumulate sufficiently in the ruthenium lattice and the second oxidation almost disappeared. On the other hand the amount of adsorbed hydrogen on the electrode surface slightly increased (a small increase in the first peak).

XRD analysis

X–ray diffraction spectra of $Ru_{0.3}Ti_{0.7}O_2$ layer are shown in Figure 10. The comparison of registered peaks with tabulated peaks of RuO_2 and TiO_2 – rutile indicates that prepared $Ru_{0.3}Ti_{0.7}O_2$ layer is fine–grain crystalline solid solution of RuO_2 and TiO_2. The parameters of

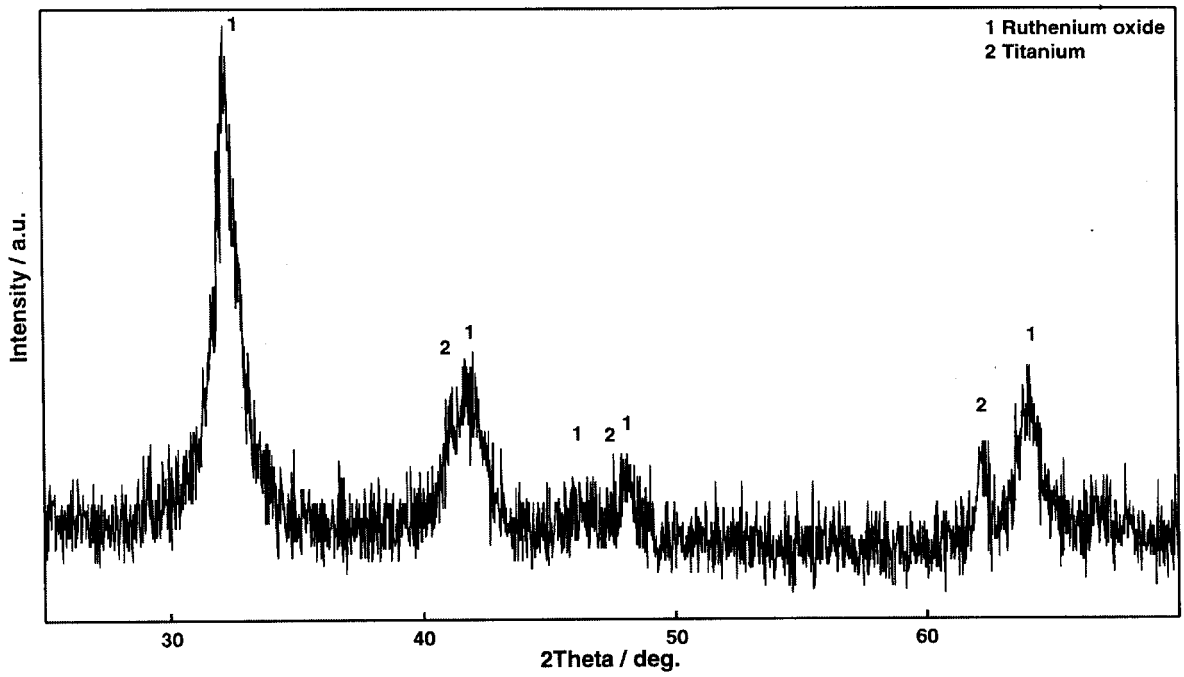

Figure 10. XRD patterns of $Ru_{0.3}Ti_{0.7}O_2$ electrode before cathodic polarization.

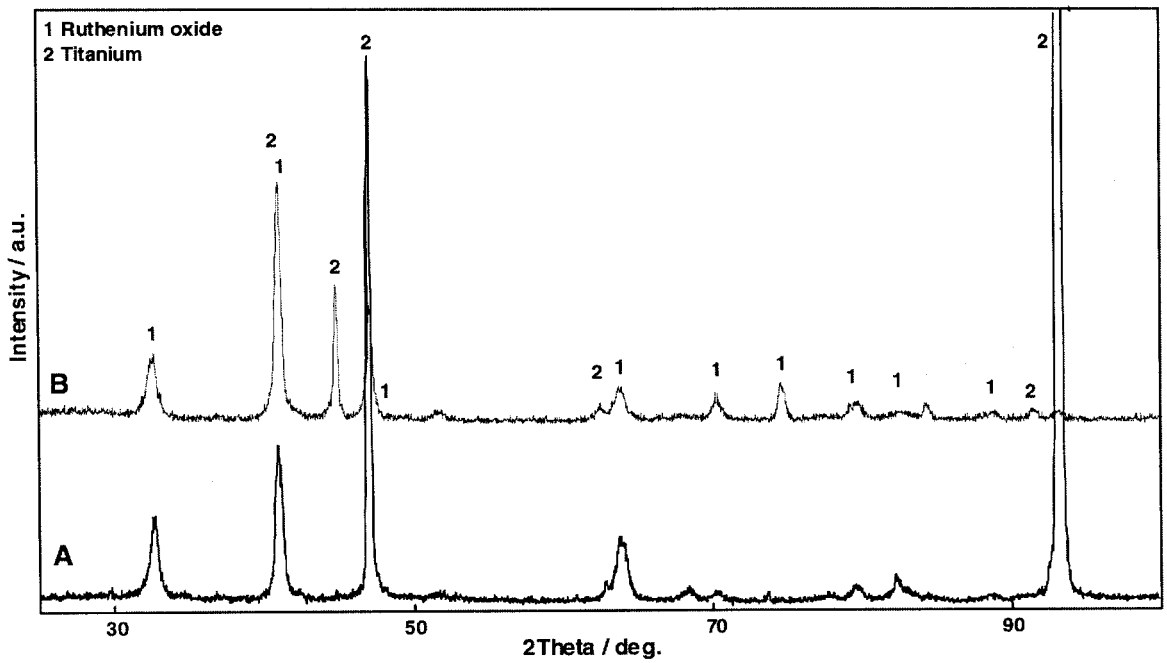

Figure 11. XRD patterns of RuO_2 electrodes deposited on Ti wire (18 layers). Curve B – before cathodic loading, Curve A – after 57 h of cathodic loading by I = 0.25 A cm^{-2}.

tetragonal lattice are: a=b=4.54, c=3.003. For the comparison the tabulated parameters of pure components are: RuO_2 – a=b=4.4994, TiO_2 – rutile – a=b=4.5933 and c=2.5992.

X–ray diffraction patterns of RuO_2/Ti electrode (18 layers, calcination 2h at 450°C on air) are shown in Figure 11. Curve **B** represents X–ray patterns of the electrode before cathodic loading, Curve **A** that after loading of the electrode by the cathodic current density I = 0.25 A cm^{-2} for 57 h. Diffraction spectra of RuO_2 (1) and titanium (2) are observed in both curves. The comparison of RuO_2 diffraction peaks of electrodes before and after cathodic loading shows that there are no notable changes of RuO_2 lattice. On the other hand there are great changes of Ti diffraction peaks of the electrode after the cathodic loading. There are no peaks

at $2\Theta \approx 45^{o}$ and 62.5^{o} and the peaks at $2\Theta \approx 67^{o}$ and 93° are extremely high. These changes are caused by the fact that during hydrogen evolution reaction hydrogen penetrates though RuO_2 layer to the basis titanium. Here hydrogen reacts with titanium forming titanium hydride. As the titanium hydride lattice differs significantly from the original titanium lattice, an appreciable stress arises in the titanium wire. After finishing cathodic loading of the electrode and withdrawing it from the solution, the decomposition of titanium hydride occurred. By this way a newly formed titanium layer is characterised by strong stresses which cause the observed changes of peak heights.

DISCUSSION

It was stated in the introductory part that hydrogen evolution on RuO_2 oxide electrode enhanced the electrode activity for this reaction. The increase in the activity was larger by up to one order of magnitude [8]. The activity increase was accompanied by the enlargement of the electrode surface by the factor 1.3 to 2.0 [20]. It followed from Figs. 1 and 2 and also from the Table 1 that the increase in the activity of electrodes and also changes of electrode surface area in our work were substantially greater than those given in the literature. The difference was caused evidently by the fact that we studied the HER on RuO_2 electrodes for considerably longer time (up to 350 h) than others. It followed further from Figs. 1 and 2 that the activity increased extremely after short–term oxidation of RuO_2 electrode at the potential around $E \approx 1.0$ V. It is necessary to note, however, that this activation is effective with electrodes only, which have been previously cathodically polarized for approximately 10 h at least. The anodic activation of freshly prepared RuO_2 electrode was without effect. On the other hand a high activity after the anodic activation was not long–term stable. After again loading by cathodic current (current density $I = 0.25$ A cm^{-2}) the activity of electrode continuously decreased. The increase in the negative potential with continued cathodic polarization was the faster the shorter time the electrode was loaded by cathodic loading before the anodic activation. In the extreme case, the polarization curve of the RuO_2 electrode deposited on gold wire and loaded for 350 h by current density $I = 0.25$ A cm^{-2} was identical with that registered immediately after anodic activation. The RuO_2 layers deposited on the titanium wire were less stable than that deposited on Au wire. The decrease in the activity for the HER was observed not only at electrodes anodically activated but also at electrodes which were loaded cathodically only. The activity of these electrodes, after reaching its maximum, decreased with continuing cathodic loading. The degradation of the activity was caused apparently mainly by mechanical effects. The microscopic examination (SEM) showed that hydrogen evolution caused crazing of the surface. With continued cathodic polarization the cracks broadened and parts of RuO_2 layer began to fall out of the surface. In the final phase the bare surface of titanium was observed even by eyes. It is obvious that the hydrogen evolution on RuO_2 electrodes caused permanent irreversible changes of RuO_2 layer. There is a question if these changes were caused by a mechanical action of evolved hydrogen bubbles only or some changes in the composition of these layers also occurred. The XPS measurements showed that ruthenium oxide is not reduced into metallic ruthenium during hydrogen evolution on RuO_2 electrodes, because X–ray photoelectron spectrum does not contain any bands of the metallic ruthenium, even in the case, when the RuO_2 electrode was placed into XPS apparatus immediately after the hydrogen evolution without any contact with air [8]. On the other hand XRD [23] and XAFS [22] measurements showed that the RuO_2 lattice was changed with Ru–O bond lengthening during the HER. The lengthening of lattice parameters was explained by the insertion of hydrogen in the RuO_2 layer [23]. The insertion of hydrogen in the RuO_2 layer during hydrogen evolution confirms also voltammetric curves Figures 5–8 and also the results of XRD measurements. Fig. 7 shows that an oxidation peak at a potential around 0.5 V appeared. It was more pronounced with increasing time of the cathodic polarisation and it shifted to more positive potentials with increasing of its height. On the other hand this peak disappeared on VCs registered immediately after the anodic potential, as it apparent from Fig. 8. Similar peak was observed on VCs of Ru electrodes, which were cathodically polarized for longer time than 18 hours (Fig. 8). These voltammetric curves gave the evidence of the hydrogen insertion in the RuO_2 and Ru layers. The insertion of hydrogen in RuO_2 was also confirmed by XRD analysis. Observed a surface stress of titanium wire with RuO_2 layer after long–term cathodic polarisation was evidently caused by the formation of titanium hydride. Hydrogen inserted through the RuO_2 layer to the titanium substrate was also responsible for the deformation of VCs of long term polarised electrodes (Fig. 6). Such deformation was not observed on RuO_2 electrodes deposited on Au wire. It is evident that the degradation of the RuO_2 layers during the HER is caused not only by the mechanical action of evolved hydrogen bubbles but also by the changes of the volume of the RuO_2 layer and by the change of the volume of the titanium substrate. The RuO_2 layers deposited on the Au substrate were therefore more stable than those deposited on the Ti substrate as the Au substrate did not absorb hydrogen.

It followed from the Table 1 that the increase in the activity of the ruthenium oxide electrodes polarized cathodically for short time only was caused mainly by the increase in the surface area of electrodes. The increase in the activity of the electrodes polarized cathodically for long–term (mainly of those with RuO_2

deposited on Au wire) was much greater than the corresponding increase in the surface area, however. The increase in the activity for the HER was accompanied by the change of the VCs – Figures 7 and 8, that is apparent mainly in the anodic branches. There appeared two oxidation peaks at E_p around 0.15 V and at E_p higher than 0.5 V. I suppose that the peak at E around 0.15 V represents the oxidation of adsorbed hydrogen, while that at E_p higher than 0.5 V represents the oxidation of absorbed hydrogen. Data of the activity for the HER (expressed as the potential of the electrode at I = 0.25 A cm^{-2} (geometric surface area)), given in the legend for the illustration, show that there is some relation between the activity and the ability of electrodes to ad– and/or absorb hydrogen. The comparison of Figures 7 and 8 and the corresponding data in the legend shows that mainly absorbed hydrogen in RuO_2 considerably influences the activity for the HER. It follows from the comparison that the oxidation of electrodes at potentials between 0.7–1.0 V causes the oxidation of absorbed hydrogen (it appeared by disappearing or lowering of the peak at E > 0.5 V). The oxidation simultaneously causes the increase in the activity for the HER and the increase in the peak corresponding to the hydrogen adsorption. (For the comparison the potential of the electrode polarized for 40 hours at I = 0.25 A cm^{-2} at the same I was E = –0.186 V and – 0.100 V, before and after the oxidation, respectively). It can be therefore concluded that hydrogen absorbed in the RuO_2 layer changes the physical–chemical properties of the electrode.

It follows from Figs 7–9 that VCs for the RuO_2 and Ru electrodes are similar. The hydrogen absorption in the Ru layer proceeded more quickly than in RuO_2, however. The considerable oxidation peak of absorbed hydrogen appeared already after 1 h of loading by cathodic current density I = 0.25 A cm^{-2}. The hydrogen absorption in the Ru layer is also accompanied by the decrease in the activity for the HER.

The behaviour of the RuO_2 electrodes at long–term cathodic loading demonstrates that the RuO_2 electrodes are not sufficiently stabile. We therefore prepared the composite layer $Ru_{0.3}Ti_{0.7}O_2$ with the aim to gain the electrode with the high activity for the HER and enough resisting to the destroying action of evolving hydrogen and also of inserting atomic hydrogen. Experimental results with this electrode showed that the requisite aim was not fulfilled. The initial activity of $Ru_{0.3}Ti_{0.7}O_2$ was comparable with that of the RuO_2 electrodes. The long–term stability of these electrodes was even worse than that of the RuO_2 electrodes, however. The activity of $Ru_{0.3}Ti_{0.7}O_2$ electrodes began to decrease already after about 20 hours of cathodic loading by I = 0.25 A cm^{-2}.

CONCLUSION

The initial activity of the RuO_2 electrodes for the HER, related to the real surface area, prepared by various methods was comparable. The initial increase in the activity after cathodic loading was caused mainly by the increase in the real surface area. Further more pronounced increase in the activity was caused by the changes of physical–chemical properties of the RuO_2 electrodes. The changes were caused by the absorption of hydrogen in the RuO_2 layer. Insertion of hydrogen in the RuO_2 layer caused lengthening of the RuO_2 lattice parameters and by this way shortening of the life–time of the electrode layer.

Metallic Ru electrodes were very active for the HER at beginning of cathodic loading. During the prolonged hydrogen evolution hydrogen absorbed in the electrode material and the activity of Ru electrodes considerably decreased.

ACKNOWLEDGEMENT

This work was supported by Grant Agency of the Czech Republic, project No. 104/00/1009.

REFERENCES

[1] O. De Nora, Chem. Eng. Tech., **42** (1970) 222.

[2] O. De Nora, Chem. Eng. Tech., **43** (1971) 182.

[3] J. Divisek, in Electrochemical Hydrogen Technologies, Electrochemical Production and Combustion of Hydrogen, H. Wendt, Editor, p. 137, Elesevier, New York (1990).

[4] S. Trasatti in Advances in Electrochemical Science and Engineering, Vol. 2, H. Gerisher and C.W. Tobias, Editors, p. 1 VCH, New York (1992).

[5] E.R. Kötz, S. Stucki, J. Appl. Electrochem., **17** (1987) 1190.

[6] J.C.F. Boodts, G. Freegonara, S. Trasatti in Performance of Electrodes for Industrial Electrochemical Processes, F. Hine, J.M. Fenton, B.V. Tilak and J.D. Lisius, Editors, PV 89–10, p. 135, The Electrochemical Society Proceedings Series, Pennington, NJ (1993).

[7] M. Blouin, D. Guay in Electrode Materials and Processes for Energy Storage and Conversion, S. Srinivasan, D.D. Macdonald, A.C. Khandkar Editors P.V. 94–23 p. 396 The Electrochemical Society Proceedings Series, Pennington, NJ (1994).

[8] M. Blouin, D. Guay, J. Electrochem. Soc., **144** (1997) 573.

[9] J.C.F. Boodts, S. Trasatti, J. Appl. Electrochem., **19** (1989) 225.

[10] A. Cornell, D. Simonsoson, J. Electrochem. Soc., **140** (1993) 3123.

[11] A. Cornell, D. Simonsoson, Proceedings of the Symposia on Chlor–Alkali and Chlorate Production, T.C. Jeffrey and K. Ota Editors PV 93–14, p. 191, The Electrochemical Society Proceedings Series, Pennington, NJ (1993).

[12] H. Chen, S. Trasatti, J. Appl. Electrochem., **23** (1993) 559.

[13] T.C. Wen, C.C. Hu, J. Electrochem. Soc., **139** (1992) 2158.

[14] N. Spataru, J.G., LeHelloco, R. Durand, J. Appl. Electrochem., **26** (1996) 397.

[15] L. Burke, O.J. Murphy, J.F. O'Neil, J. Electroanal. Chem., **96** (1979) 19.

[16] E.R. Kötz, H.J. Lewerenz, P. Bruesh, S. Stucki, J. Electroanal. Chem., **150** (1983) 209.

[17] S. Ardizone, G. Fregonara, S. Trasatti, J. Electroanal. Chem., **266** (1989) 191.

[18] D. Miousse, A. Lasia, J. New Mater. Electrochem. Syst., **2** (1999) 71L.

[19] B.V. Tilak, V.I. Birs J. Wang, C.P. Chen, S.K. Rangarajan, J. Electrochem. Soc., **148** (2001) D 112.Y

[20] L. Chen, D. Guay F.H. Pollak, F. Levy, J. Electroanal. Chem., **429** (1997) 185.

[21] Y. Takasu, Y. Murakami, Electrochim. Acta, **45** (2000) 4135.

[22] Y. Mo, W.B. Cai, J. Dong P.R. Carey, D.A. Schercon, Electrochem. Solid– State Lett., **4** (2001) E37.

[23] C. Chabanier, E. Irissou, D. Guay, J.F. Pelletier, M. Sutton, L.B. Lurio, Electrochem. Solid – State Lett., **5** (2002) E40.

[24] C. Forti, P. Olivi, A.R. de Andrade, Electrochim. Acta, **47** (2001) 913.

[25] I. Paseka, Applied Catalysis A: General, **207** (2001) 257.

IVO PASEKA

Ivo Paseka born in 1933 in Prerov, Czech Republic. Between 1952 and 1957 study at the Prague Institute of Chemical Technology, Institute of Inorganic Technology. Ph.D. study at the Institute of Inorganic Chemistry, Czechoslovak Academy of Sciences. Ph.D. obtained at that Institute in 1961. Since that year he worked at that Institute as a scientist in the group of technical electrochemistry. Since 1977 he was the head of this group until 1995. Since 1996 until now he has worked as the Senior scientist in the Department of Solid State Chemistry of the Institute of Inorganic Chemistry of the Academy of Sciences of the Czech Republic, now situated in a research centre in ež near Prague.

Main research activities: electrocatalytic materials for hydrogen and oxygen evolution, electroreduction of nitric oxide, non–metallic materials for alkali amalgam decomposition, hydrogenation and electroreduction of unsaturated compounds, using electrochemical methods in the characterization of some metal catalysts, properties of amorphous electrocatalysts (mainly NiP_x and NiS_x), electrochemistry of Ru and RuO_2 materials, synthesis of special magnetic materials.